MASARYKOVA UNIVERZITA
Přírodovědecká fakulta

Bc. Nikola Heroldová

Low-temperature alteration of metamict Y,REE-Nb,Ta,Ti minerals

Rešerše k diplomové práci

Vedoucí práce: Mgr. Radek Škoda, Ph.D.

Brno 2011

Table of contents

1. Introduction

Minerals containing U and Th commonly occur in amorphous state although they were formed as crystalline. These phases are called metamict minerals and represent particular groups of oxides, phosphates and silicates, most of them are very significant accessory minerals. The term metamict is derived from two latin words: meta=after and mikto=mixing. This name is related to changes, which affected them. All of these minerals contain radioactive elements. Radioactive decay of these elements is responsible for deformation or destruction of original mineral structure. Radiation effects from α-decay in crystalline oxides are well known to result in amorphization and consequent changes of physical and chemical properties (Ewing et al. 1995).

2. The metamictization processes

Metamictization of minerals is a result of two counteracting processes: radiation damage accumulation and radiation damage annealing. Some minerals like zircon, titanite, and Y,REE-Nb,Ta.Ti oxides commonly become metamict, whereas minerals like monazite and apatite preserve their crystalline state, even if they experienced similar radiation doses (e.g. Nasdala et al. 2001). The main reason for the distinct behavior of these minerals is caused by different structure related temperature-dependencies of their annealing rates (Meldrum et al. 1998). Processes leading to metamictization and overall impact on the properties of minerals are described in following chapters.

2.1. Radiation effects

Radiation effects from α-decay in crystalline oxides in many cases result in amorphization, macroscopic swelling and order-of-magnitude increases in dissolution rates (Ewing et al. 1995, 1996, Weber et al. 1998, Geisler et al. 2005a, Pöml et al 2007).

The current understanding regarding radiation effects and radiation damage processes in crystalline phases is summarized below.

2.1.1. Radiation damage processes

The origin of natural radiation causing metamictization is in α-decay events of U and Th decay chains. The α-decay releases alpha particles with energies of 4.5 to 5.8 MeV, and recoil nuclei with energies of 70 to 100 KeV.

The α-particles and α-recoils interacting with the atomic structure lead to radiation damage. These interactions transfer the energy to electrons (ionization and electronic excitation) and to atomic nuclei by ballistic processes involving elastic collisions. An α-particle deposits its energy mainly by ionization processes, whereas α-recoil looses most of its energy during elastic collisions. An α-particles are able to interact only at the far end of its path through elastic collision with lattice atoms followed by generating atoms displacements (Nasdala et al. 2001). Changes in the microstructure with increasing dose can be observed by using high resolution TEM (see Fig. 1).

Particles emitted by radioactive decay can also have a significant chemical effect on the host material. The α-particles looses most of its energy by ionization processes in a range of 16 to 22 μm producing hundreds of atomic displacements (mainly at the end of α-particle range) that form Frenkel pairs. However, the most displacements are caused by ballistics processes of α-recoil despite of its lower energy. During α-decay event, α-particle and α-recoil are released in opposite directions and form damage regions separated by several micrometers (Ewing et al. 2004). Nasdala et al. (2001) made Monte Carlo simulations on zircons, which revealed that single α-particle generates about 120-130 Frenkel type defect pairs, whereas the recoil nuclei can generate 600-1200 Frenkel defect pairs.
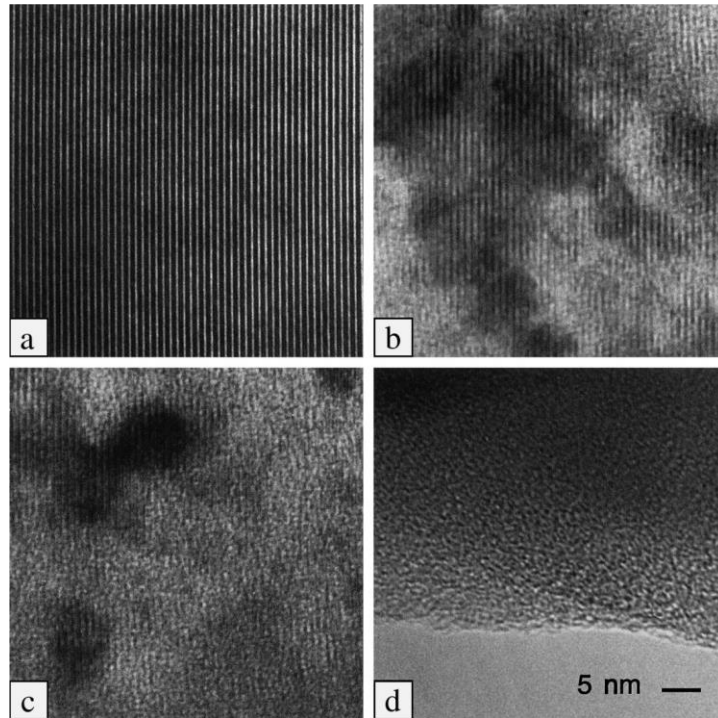
Figure 1. High resolution TEM images of crystalline-amorphous transformation in Ta-rich pyrochlore subgroup mineral (microlite) from the Harding pegmatite. (a) highly crystalline sample, $D=0.2 \times 10^{16}$ α mg^{-1}. (b) Partially damaged sample, $D=3.5 \times 10^{16}$ α mg^{-1}. (c) Heavily damaged sample, $D=9.6 \times 10^{16}$ α mg^{-1}. (d) Completely amorphous sample, $D=13.8 \times 10^{16}$ α mg^{-1} (Lumpkin 2001).

2.2. Damage production

The most important parameters affecting radiation damage in materials is displacement energy, E_d, representing the minimum kinetic energy necessary to displace an atom from its original site. This parameter is fundamental for quantifying the number of displaced atoms produced in irradiated materials (Weber et al. 1998). The relationship between E_d and minimum electron energy - E_e, is described by equation below (Kelly 1966)

$$E_d = 2E_e(E_e + 2m_ec^2)/Mc^2,$$

where m_e is electron mass, M is the mass of the displaced ion and c is velocity of light.

2.3. Volume changes

During metamictization original grains swell and decrease their density. This macroscopic swelling is commonly accompanied by radial cracks in the host rock around the grain, typically around allanite and zircon.

Volume changes in crystalline phases can result from the accumulation of defects in crystalline structure, solid-state phase transformations (e.g. amorphization) and microstructural defects (e.g. He gas bubbles, voids, microcracks and dislocations). The large differential changes in volume can result in high internal stresses and may cause microcracking, segregation and increased dissolution rates. The large volume changes significantly affect atomic bonding, local coordination, and pathways for ion exchange (Weber et al. 1998).

Weber et al. (1998) also proposed a general equation for total macroscopic swelling $\Delta V_m/V_0$:

$$\Delta V_m/V_0 = f_c \Delta V_{uc}/V_0 + f_a \Delta V_a/V_0 + F_{ex}$$

where f_c is the mass fraction of crystalline phase, f_a is the mass fraction of amorphous phase, $\Delta V_{uc}/V_0$ is the unit cell volume change associated with the amorphized state, and F_{ex} is the volume fraction of extended microstructures (e.g., voids, microcracks, pores and bubbles). In most studies, F_{ex} is negligible an equation reduces to that proposed by Weber (1993).

2.4. Mechanical properties

The toughness of fractures increases with cumulative dose, and after reaching the maximum, it slightly decreases (Ewing et al. 1995). At lower doses, microstructure consists of amorphous phase in the crystalline matrix. It can reduce the propagation of cracks and increase the fracture toughness. At high doses, amorphous phase becomes the dominant matrix with crystalline remnants. The fracture toughness slightly decreases when internal stress reveals (Ewing et al. 2004).

2.5. Amorphization

Self-radiation damage from α-decay events results in a crystalline to amorphous transformation. The exact nature of the amorphization process is not well defined but most likely amorphization appears to occur heterogeneously by several mechanisms:

a) directly in the α-recoil displacement cascade

b) from the accumulation defects due to overlap of α-recoil cascades

c) phenomena involving more than one process

Amorphization results in atomic density decrease and changes in local and long-range structure. Amorphization becomes more difficult with increasing temperature and occurs only under critical temperature. Once the amorphized state is formed, it is stable under further irradiation (Weber et al. 1998).

Radiation-induced amorphization of crystalline materials leads to aperiodic structures with large changes in volume. Such aperiodic structures formed in U-, Th-containing minerals as a result of α-decay, are referred to as metamict (Stackelberg and Rottenbach 1939).

Salje et al. (1999) defined two percolation points for amorphization. Below the first percolation point, when amorphous regions are isolated and surrounded by crystalline matrix, the swelling of amorphous domains is small or even negative. At this stage, amorphous regions are compressed by crystalline matrix. Above the second percolation point, when matrix consist mainly of amorphous stage, the amorphous regions are free to swell. Between these two percolation points, the material contains both already percolated amorphous regions and amorphous regions still surrounded by crystalline regions (Ríos et al. 2000).

With increasing amorphization decreases a crystallinity, which can be observed in changing X-ray powder diffraction pattern. The first stage of amorphization is characterized by sharp Bragg diffraction maxima with a minor contribution from the diffuse-scattering component. In later stages, the intensity of Bragg maxima decreases and becomes asymmetric due to increased contributions from the diffuse-scattering component (Murakami et al. 1991).

2.6. Annealing and recrystallization

A crystal structure of metamict minerals can be restored by annealing. The time for recrystallization increases with intensity of prior metamictization. Generally in experiments, metamict minerals are heated for several hours, usually for more than one day, at temperatures ranging from 400°C to 1000°C. Such a heat treatment can induce the

recrystallization of radiation-damaged structure. (Tomašić et al. 2008). Hydrothermal conditions are also efficient for the recrystallization of heavily metamictized minerals.

In experimental work of Tomašić et al. (2004) has been studied an influence of heat on aeschynite-Y and polycrase-Y. During 24 hours of heating in muffle furnace, the diffraction maxima became sharper and more intense indicating reconstruction of crystal structure. Both minerals started gradually to crystallize at 400°C with the aeschynite structure. As the temperature raised, aeschynite was transformed to the euxenite structure. The first transition to euxenite structure appeared at 650°C (for polycrase-Y) and 800°C (for aeschynite-Y).

3. Metamict Y,REE-Nb,Ta,Ti minerals

The (Y,REE,U,Th)-(Nb,Ta,Ti) oxide minerals are mainly present in REE-enriched granitic pegmatites and A- and I-type fractionated granites. They consist of many mineral groups and species. The main groups include minerals of aeschynite, euxenite, samarskite, fergusonite and pyrochlore. These minerals are typically metamict and altered (Ercit 2005). The detailed description of individual groups is provided below.

3.1. Aeschynite

Aeschynite is a typical phase occurring in REL-REE pegmatites of euxenite subtype (Černý and Ercit 2005). Minerals from aeschynite group are metamict with brown or brownish black color. They form anhedral grains, elongated subhedral crystals and also euhedral columns. These minerals are commonly altered, accompanied with a brown halo around grains. Aeschynite is frequently replaced by secondary minerals from pyrochlore group (Škoda et al. 2006).

The general formula for aeschynite is AB_2O_6, where position A is represented by Y, REE, Ca, U and Th; and position B is occupied by Ti, Nb and Ta. (Ercit 2005). See element distribution in Fig. 2. An overview of the minerals from aeschynite group is presented in Tab. 1.

Aeschynite group minerals have ideally Pbnm symmetry, with a 10.9, b 7.5 and c 5.2 Å. The aeschynite structure prefer larger A cations than euxenite structure. Thus aeschynite group minerals have higher LREE (Y + HREE) ratio than euxenite group minerals (Ewing 1976).

8

Aeschynite group minerals	Ideal formula
Aeschynite-(Y)	$Y(Ti, Nb)_2O_6$
Aeschynite-(Ce)	$Ce(Ti, Nb)_2O_6$
Aeschynite-(Nd)	$Nd(Ti, Nb)_2O_6$
Nioboaeschynite-(Ce)	$Ce(Nb, Ti)_2O_6$
Tantalaeschynite-(Y)	$Ca, Y(Ta, Nb, Ti)_2O_6$
Vigezzite	$CaNb_2O_6$
Rynersonite	$CaTa_2O_6$

Table 2. Currently valid list of aeschynite group of minerals (Mandarino and Black 2004).
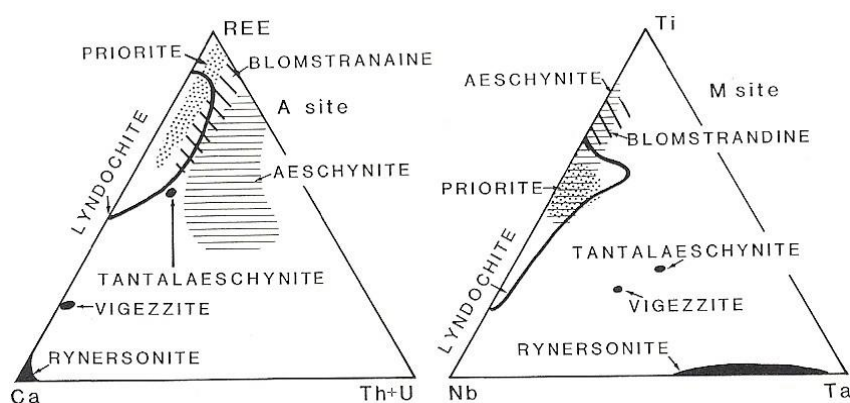

Figure 2. Distribution of atoms in both positions A and B in aeschynite group (Černý and Ercit 1989).

3.2. Euxenite

Euxenite group of minerals (Tab. 2) is similarly like aeschynite limited to pegmatites of euxenite subtype (Černý and Ercit 1989, 2005). They form isometric subhedral to euhedral grains, usually elongated to needle-shaped crystals. In general, it is almost impossible to recognize them macroscopically from aeschynite, in many cases nor from pyrochlore (Škoda et al. 2006) The general formula of euxenite is AB_2O_6. Octahedral position A is occupied by Y, REE, Ca U and Th, while hexahedral position B is occupied by Ti, Nb and Ta. More details about element distribution in euxenite is in Fig. 3. Euxenite group minerals have ideally Pbcn symmetry, with *a* 14.6, *b* 5.6 and *c* 5.2 Å (Ercit 2005).

Euxenite group of minerals	Ideal formula
Euxenite-(Y)	$Y(Nb, Ti)_2O_6$
Tanteuxenite-(Y)	$Y(Ta, Ti, Nb)_2O_6$
Polycrase-(Y)	$Y(Ti, Nb)_2O_6$
Uranopolycrase	UTi_2O_6
Yttrokrasite	$(U, Th)(Ti, Fe^{3+})_2(O, OH)_6$
Fersmite	$CaNb_2O_6$

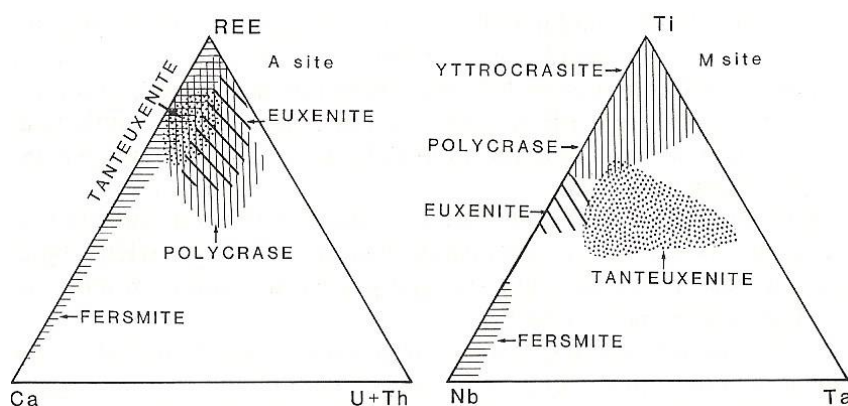Table 2. Currently valid list of euxenite group of minerals (Mandarino and Black 2004).

Figure 3. Distribution of atoms in both positions A and B in euxenite group (Černý and Ercit 1989).

3.3. Fergusonite

The general formula of fergusonite is ABO_4, where position A is occupied by Y and REE and position B is occupied by Nb and Ta (see Fig. 4). Fergusonite has predominantly tetragonal habit with a scheelite type structure (Černý and Ercit 1989, Ercit 2005). Individual minerals from fergusonite group of minerals are presented below (Tab. 3).

Fergusonite group of minerals	Ideal formula
Fergusonite-(Y)	$YNbO_4$
Beta-fergusonite	$YNbO_4$
Formanite	$YTaO_4$

Table 3. Currently valid list of fergusonite group of minerals (Ercit 2005).

Other mineral analogues from this group of minerals are beta-fergusonite-(Y), Ce and Nd analogues of fergusonite-(Y). However, these signification was used without approval of IMA (Ercit 2005).

Fergusonite-Y is tetragonal and has ideally *a* 5.3, *c* 10.9 Å, space group I4$_1$/a. The monoclinic members (beta-fergusonite and formanite) have ideally a 5.3, b 11, c 5.1, β 95°, space group I2/c. Compare to samarskite, fergusonite structure seem to be more stable for higher values of the A:B radius ratio (Ercit 2005).
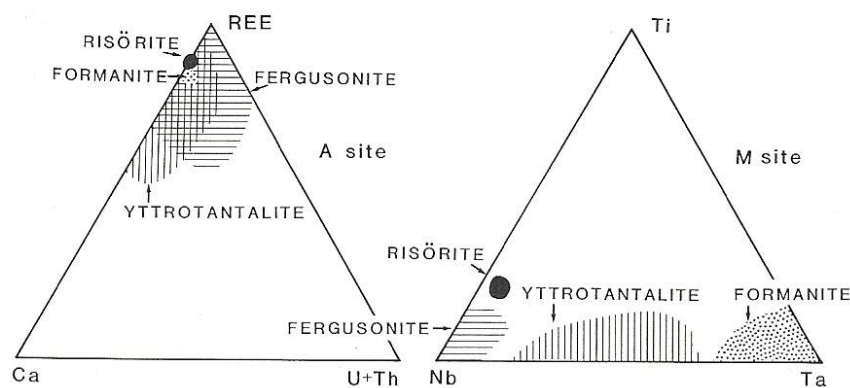

Figure 4. Distribution of atoms in both positions A and B in fergusonite group (Černý and Ercit 1989).

3.4. Samarskite

Samarskite (Tab. 4) often forms elongated crystals and its aggregates can be more than X cm large. Samarskite has brownish black color with vitreous or greasy luster and frequently contains microscopic grains of fergusonite. The general structural formula of samarskite group of minerals is ABO$_4$. (Ercit 2005) Position A is occupied by Th, U, Y, Mn, Ca, Pb, REE, Na, Fe2+ and position B is occupied by Nb, Ta, Ti, Zr, Al, Fe^{3+} (Lumpkin and Ewing 1987). More details in element distribution is in Fig. 5. All members of samarskite group minerals have ideally monoclinic P2/c, with *a* 5.7, *b* 9.9 and *c* 5.2 Å, β 94° (Ercit 2005).

Samarskite group of minerals	Ideal formula
Samarskite-(Y)	$(Y, Ca, Fe)NbO_4$
Calcio-samarskite	$(Ca, Y, U)NbO_4$
Ishikawaite	$(U, Fe, Y, Ca)NbO_4$

Table 4. Currently valid list of samarskite group of minerals (Hanson et al. 1999, Warner and Ewing 1993).
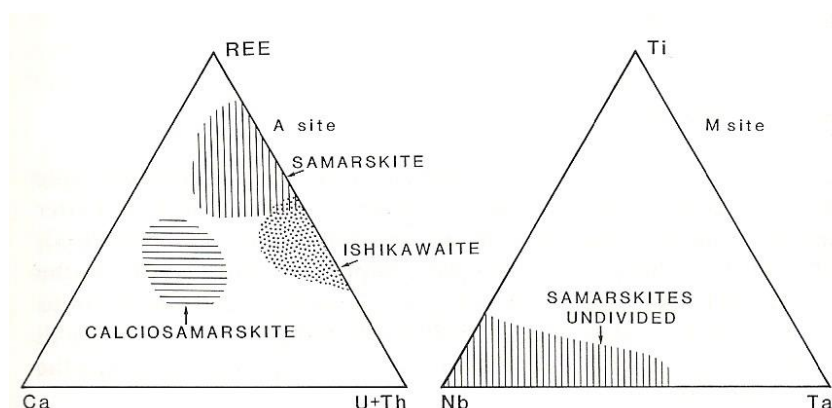

Figure 5. Distribution of atoms in both positions A and B in samarskite group (Černý and Ercit 1989).

3.5. Pyrochlore

Pyrochlore crystallizes in a cubic system (Fd3m, *a* 10.4 Å) and the general formula for these minerals is $A_{2-m}B_2X_{6-w}Y_{1-n}$, where position A represents cations in hexahedral coordination (e.g. Na, Ca, Sr, Pb^{2+}, Sn^{2+}, Sb^{3+}, Y, U, □, H_2O), position B represents cations in octahedral coordination (Ta, Nb, Ti, Sb^{5+}, W), X (O) and Y is occupied by OH^-, F, O, □, H_2O. A wide variety of large, mostly mono- to trivalent cations are possible in position A, resulting in a high number of endmembers. Crystallochemistry of pyrochlore is very complicated due to possible numbers of vacancies in positions A, X and Y. Depending on ions at A, B and Y sites, five main groups were defined by Atencio et al. (2010):

1. Pyrochlore, if Nb is the dominant M^{5+} cation in the octahedral site

2. Microlite, if Ta is the dominant M^{5+} cation cation in the octahedral site

3. Roméite, if Sb is the dominant M^{5+} cation cation in the octahedral site

4. Betafite, if Ti is the dominant M^{4+} cation cation in the octahedral site

5. Elsmoreite, if W is the dominant M^{6+} cation cation in the octahedral site

The most important metamict mineral species occur mainly in REE rich pegmatites and fractionated granites. Previously existing minerals described in Hogarth (1977) have been discredited and therefore it is necessary for some other minerals to be reevaluated.

The current list of valid species of the pyrochlore supergroup minerals is listed in the Tab. 5.

Pyrochlore group of minerals	Ideal formula
Oxycalciopyrochlore	$Ca_2Nb_2O_6O$
Hydropyrochlore	$(H_2O, \square)_2Nb_2(O,OH)_6(H_2O)$
Hydroxykenomicrolite	$(\square,Na,Sb^{3+})_2Ta_2O_6(OH)$
Oxystannomicrolite	$Sn_2Ta_2O_6O$
Oxystibiomicrolite	$(Sb^{3+},Ca)_2Ta_2O_6O$
Hydroxycalcioroméite	$(Ca, Sb^{3+})_2(Sb^{5+},Ti)_2O_6(OH)$
Hydrokenoelsmoreite	$\square_2W_2O_6(H_2O)$

Table 5. Valid list of pyrochlore group of minerals according to Atencio et al. (2010).

4. Hydrothermal alteration of metamict minerals in the nature compared with experiments

Alteration processes have been divided into primary and secondary types by Van Wambeke (1970) and Ewing (1975). Primary alteration is hydrothermal and is associated with host rocks emplacement. This type of alteration occurs prior to significant radiation damage and results in either change in composition or replacement by one or more phases. Secondary alteration is near-surface phenomena (weathering) and occurs after crystal structure has been changed to aperiodic (metamict). Secondary alteration in pyrochlore leads to significant increases in vacancies due to increased hydration and leaching of A-site cations and Y-site anions (Lumpkin and Ewing 1992).

Understanding of alteration processes of potential nuclear waste form materials in aqueous media is important for the prediction of their long-term stability in nuclear repository. This stability is very important since any contact with aqueous fluids in repository will be the most effective process to avoid radionuclide release into environment (Geisler 2005b).

When a fluid interacts with the solid phase, several reactions are possible. These reaction mechanisms depends on the physicochemical conditions of the fluid and the structural and thermodynamic properties of the solid phase, for instance, porosity of the structure, defect concentration, degree of amorphization and elastic strain. One of the processes that can occur is breaking of cation-oxygen bonds followed by stoichiometric dissolution. This dissolution is associated with precipitation of thermodynamically more stable phase at the moving front. However, when fluid is presence in solid state, then interaction with solid parent phase is controlled by diffusion-reaction processes (also known as leaching reactions; Geisler et al. 2005a).
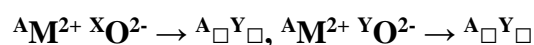
Detailed studies of the alteration of natural pyrochlore samples provide an information about long-term behavior of pyrochlore compounds under geological conditions. Studies of natural pyrochlore have been provided by Lumpkin and Ewing (1995, 1996). Natural pyrochlore exhibits alteration effects that are transitional between primary (hydrothermal) and secondary (near surface) alteration. More precisely, microlite, pyrochlore and betafite leach from hydrothermal conditions (maximum 650°C and 5 kbar) to near surface conditions (weathering environment). Thus fluids range from dense, supercritical magmatic fluids to mixed magmatic-meteoric fluids, to groundwater of low ionic strength. The A-site cations mobility is limited by valence and ionic radius constrains. The least mobile A-site cations of these minerals are U^{4+}, Th^{4+} and REE^{3+}. In PTX conditions, the alteration is influenced by grain size, prior radiation damage and microfracturing, volume and flow rate of fluids and total exposure time. In laterite horizons and weathering environment, rate of ion exchange exceeds the total dissolution rate, controlled by stability of octahedral framework when occupied by Nb, Ta and Ti (Lumpkin and Ewing 1995).

In comparison to this study, hydrothermal experiments of pyrochlore have been made by Geisler et al. (2005a). They performed experiments with crystalline microlite and heavily self-irradiation-damaged betafite in acidic solution at 175°C for 14 days. These experiments have shown, that crystalline Ti-based pyrochlore is more stable in aqueous solution than Ta-based natural pyrochlore. But in general, these experimental observations are similar to

natural samples observations. They indicate that the processes of the fluid-pyrochlore interaction are strongly influenced by self-irradiation structural damage.

Synthetic and natural Ti-based (betafite-Y) pyrochlore samples have been also compared in Pöml et al. (2007). The results were produced under relatively extreme experimental conditions showing the similarities between nature and experiments. After experiments (in 1M HCl solution for 3 days, involving ^{18}O as a tracer), both samples were mainly transformed into rutile with subordinate anatase. In the natural sample, the additional phase (aeschynite) appeared. During alteration process the REEs, Y and most of the U were removed from the amorphous betafite, leaving behind Ti, Nb and Ta, allowing the growth of anatase and anatase-to-rutile transformation to occur. In both cases ^{18}O was enriched in reaction products. Compared to the natural sample, the reaction advanced deeper in the crystalline sample, because the ceramic polycrystalline and fluid could migrate along the grain boundaries.

From the experimental studies has been concluded that pyrochlore compounds dissolve nonstochiometrically by forming an alteration layer (also leached layer) as a result of hydration and loss of A-site cations. The chemical alteration reactions in natural pyrochlore are provided by Lumpkin (2001) and Lumpkin et al. (2004) as a substitution reaction in the form:

$$^{A}M^{2+}\,^{X}O^{2-} \rightarrow {}^{A}\square\,^{Y}\square, \quad {}^{A}M^{2+}\,^{Y}O^{2-} \rightarrow {}^{A}\square\,^{Y}\square$$

and in F containing pyrochlore: $\quad ^{A}M^{+}\,^{Y}F^{-} \rightarrow {}^{A}\square\,^{Y}\square,$

where M and $\square$ represent an A-site cation and a vacancy, and arrow indicates "replaced by".

Similar experiment has been done for metamict fergusonite by Ruschel et al. (2010). The fluid driven alteration seemed to be controlled by accessibility of micro areas to the alteration fluid through fractures, serving as fast migration pathways. One of the important observations was relatively small changes in U and Th contents compare to other elements (e.g. Si, Ca and most REE). This suggests that the radionuclides are not necessarily leached-out preferentially in a fluid driven replacement reaction in fergusonite.

References

Atencio D., Andrade M. B., Christy A. G., Girré R., Kartashov P. M., (2010): Pyrochlore subgroup of minerals: nomenclature, The Canadian Mineralogist, 48, 673-698

Černý P., Ercit T. S., (1989): Mineralogy of Niobum and Tantalum: Crystal Chemical Relationships, Pagarenetic Aspects and Their Economic Implications, In: P. Möler, P. Černý, F. Saupé (ed.): Lanthanides, Tantalum and Niobium, 27-79.

Černý P., Ercit T. S., (2005): Classification of granitic pegmatites, Canadian Mineralogist, 43, 2005-2026.

Ercit T. S. (2005): Identification and alteration trendes of granitic-pegmatite-hosted (Y,REE,U,Th)-(Nb,Ta,Ti) minerals: A statistical approach, The Canadian Mineralogist, 43, 1291-1303.

Ewing R. C. (1975): Alteration of melamict, rare-earth, AB_2O_6-type Nb-Ta-Ti oxides, Geochimica et Cosmochimica Acta, 39, 521-530.

Ewing R. C. (1976): Mineralogy of metamict rare earth AB2O6-type niobium-tantalum-titanium oxides. Ph.D. thesis, Stanford university, Stanford, California

Ewing R. C., Weber W. J., and Clinard F. W., (1995): Jr., Prog. Nucl. Energy, 29, 63

Ewing R. C., Weber W. J., and Lutze W., (1996): in Disposal of Weapons Plutonium, edited by E. R. Merz and C. E. Walter (Kluwer Academic, The Netherlands), 65.

Ewing R. C., Weber W. J., and Lian J., (2004): Nuclear waste disposal - pyrochlore (A2B2O7): Nuclear waste form for the immobilization of plutonium and "minor" actinides. 95, 11, 5949-5971

Geisler T., Seydoux-Guillaume A.-M., Poeml P., Golla-Schindler U., Berndt J., Wirth R., Pollok K., Janssen A., Putnis A., (2005a): Experimental hydrothermal alteration of crystalline and radiation-damaged pyrochlore. Journal of nuclear materials, 344, 17-23

Geisler T., Pöml P., Stephan T., Janssen A., Putnis A., (2005b): Experimental observation of an interface-controlled pseudomorphic replacement reaction in a natural crystalline pyrochlore. American mineralogist, 90, 1683-1687

Hanson S. L., Simmons W. B., Falster A. U., Foord E. E., Lichte F. E., (1999): Proposed nomenclature for samarskite-group minerals: new data on ishikawaite and calciosamarskite, Mineralogical Magazine, 61, 1, 27-36.

Hogarth D. D. (1977): Classification and nomenclature of pyrochlore group, American Mineralogist, 62, 403-410.

Kelly B. T. (1966): Irradiation damage to solids, Pergamon press, New York

Lumpkin G. R., Ewing R. C., (1992): Geochemical alteration of pyrochlore group minerals: Microlite subgroup, American Mineralogist, 77, 179-188.

Lumpkin G. R., Ewing R. C., (1995): Geochemical alteration of pyrochlore group minerals: Pyrochlore subgroup. American mineralogist, 80, 732-743

Lumpkin G. R., Ewing R. C., (1996): Geochemical alteration of pyrochlore group minerals: Betafite subgroup. American mineralogist, 81, 1237-1248

Lumpkin G. R., (2001): Alpha-decay damage and aqueous durability of actinide host phases in natural system, Journal of nuclear materials, 289, 136-166

Lumpkin G. R., Smith K. L., Gieré R., Williams C. T., (2004): Assessing the geochemical behavior of crystalline nuclear waste forms using natural analogues. In R. Gieré, P. Stille, Eds, Waste and environment, a geochemical perspective, Special publication, Geological Society of London, 236, 89-111

Mandarino J. A., Black M. E., (2004): Freischer's Glossary of Mineral Species, The Mineral, Record Inc., Tucson, 309.

Meldrum A., Boatner L. A., Weber W. J., Ewing R. C., (1998): Radiation damage in zircon and monazite, Geochim Cosmochim Acta. 62, 2509-2520

Murakami T., Chakoumakos B. C., Ewing R. C., Lumpkin G. R., Weber W. J., (1991): American mineralogist, 76, 1510

Nasdala L., Wenzel M., Vavra G., Irmer G., Kober B., Wenzel M., (2001): Metamictization of natural zircon: accumulation versus thermal annealing of radioactivity-induced damage, Contrib. Mineral. Petrol., 141, 125-144

Pöml P., Menneken M., Stephan T., Niedermeier D. R. D., Geisler T., Putnis A. (2007): Mechanism of hydrothermal alteration of natural self-irradiated and synthetic crystalline titanate-based pyrochlore, Geochimica et Cosmochimica Acta, 71, 3311-3322

Ruschel K., Nasdala L., Rhede D., Wirth R., Lengauer C. L., Libowitzky E., (2010): Chemical alteration patterns in metamict fergusonite, Eur. J. Mineral., 22, 425-433

Ríos S., Salje E. K. H., Zhang M., Ewing R. C., (2000): Amorphization in zircon: evidence fir direct impact damage, Journal of physics, 12, 2401-2412

Stackelberg M. V. and Rottenbach E. (1939): Z. Kristalogr. 102, 173 and 207

Salje E. K. H., Chrosch J., Ewing R. C., (1999): Is "metamictization" of zircon a phase transition?, American mineralogist, 84, 7-8, 1107-1116

Škoda R., Novák M., Houzar S., (2006): Granitické NYF pegmatity třebíčského plutonu. Acta Mus. Moraviae, Sci. Geol., 91, 129–176.

Tomašić N., Gajović A., Bermanec V., Rajić M., (2004): Recrystallization of metamict Nb-Ta-Ti-REE complex oxides: A coupled x-ray-diffraction and raman spectroscopy study of aeschynite-(Y) and polycrase-(Y), The canadian mineralogist, 42, 1847-1857

Tomašić N., Bermanec V., Gajović A., Linarić M. R., (2008): Metamict minerals: An insight into a relic structure using XRD, raman spectroscopy, SAED and HRTEM, Croatia chemica acta, 81, 391-400

Van Wambeke L. (1970): The alteration process of the complex titanoniobo-tantalates and their consequences. Neues Jahrbuch fur Mineralogie Abhandlungen, 112, 117-149.

Warner J. K., Ewing R. C., (1993) Crystal chemistry of samarskite, American Mineralogist, 78, 419-424.

Weber W. J. (1993): J. Amer. Ceram. Soc. 76, 1729

Weber W. J., Ewing R. C., Catlow C. R. A., Diaz de la Rubia T., Hobbs L. W., Kinoshita C., Matzke Hj., Motta A. T., Natasi M., Salje E. K. H., Vance E. R., Zinkle S. J., (1998): Radiation effects in crystalline ceramics fo the immobilization of high-level nuclear waste and plutonium, J. Mater. Res, 13, 6, 1447-1462